UACJ Technical Reports, Vol.1 (2014), pp. 37-44

論　文

Mechanical Properties of 7475 Based Aluminum Alloy Sheets with Fine Subgrain Structure by Warm Rolling*

Hiroki Tanaka** and Tadashi Minoda***

The effect of transition elements on grain refinement of 7475 aluminum alloy sheets produced by warm rolling was investigated. The alloy which contains zirconium instead of chromium showed ultra fine structures with stable subgrains after warm rolling at 350℃ , followed by solution heat treatment at 480℃ . The average subgrain diameter was approximately 3 μm. It became clear that zirconium in solution has the effect of stabilizing subgrains due to precipitation of fine Al_3Zr compounds during warm rolling. On the other, chromium-bearing compounds precipitate before warm rolling and they grow in relatively large size during warm rolling. The warm rolled sheets with fine subgrains have unique properties comparing to conventional 7475 aluminum alloy sheets produced by cold rolling. The warm rolled sheets as solution heat treated had subgrain structures through the thickness with a high proportion of low angle boundary less than 15°. The strength of the warm rolled sheets in T6 condition was about 10% higher than that of conventional 7475 aluminum alloy sheets. As the most remarkable point in the warm rolled sheets, the high Lankford (r) value of 3.5 was measured in the orientation of 45° to rolling direction, with the average r-value of 2.2. The high r-value would be derived from well developed β-fiber textures, especially with the strong {011}<211> Brass component. The warm rolled sheets also had high resistance to SCC. From Kikuchi lines analysis and TEM images, it was found that PFZs were hardly formed along the low angle boundaries of the warm rolled sheets in T6 condition. This would be a factor to lead to the improvement of resistance to SCC because of reducing the difference in electrochemical property between the grain boundary area and the grain interior.

Keywords: *warm rolling, aluminum-zinc-magnesium-copper, grain refinement, stress corrosion cracking*

1. Introduction

In order to use wrought aluminum alloys for structural components, it is important to improve their mechanical properties on resistance to corrosion and formability as well as strength for high reliability, good design and weight saving. It is well known in low-carbon steels that yield stress has a relation with grain size[1), 2)], and the relation can be applied to aluminum alloy sheets. Due to the fact, the grain refinement of aluminum alloy sheets is one useful method to achieve high strength. On the other hand, it was reported that the grain refinement of 7075 aluminum alloy sheets has a disadvantage on resistance to stress corrosion cracking (SCC)[3)]. It would be difficult to establish a process that can achieve the improvement of all properties mentioned above at the same time. Therefore, in practical use, some of the mechanical properties should be improved moderately according to circumstances where materials are used. In the previous study[4)], it was revealed that the control of second phase distributions and solution elements leads fine structure about 7 μm on average grain diameter in 7475 aluminum alloy sheets by cold rolling after solution heat treatment.

The objective of the present work is to form finer structure in 7475 based aluminum alloys by warm

* The main part of this paper was presented at Trans. Nonferrous Mat. Soc. China, **24** (2014), 2187-2195.

** No.3 Department, Nagoya Center Research & Development Division, UACJ Corporation

*** Extrusion & Drawing Technology Section, UACJ Extrusion Nagoya Corp.

rolling which can control subgrain stability and to clarify mechanical properties of the warm rolled sheets comparing with conventional 7475 aluminum alloy sheets produced by cold rolling.

2. Experimental procedures

Table 1 shows the chemical compositions of Al-Zn-Mg-Cu alloys used in this study. The mark M means an 7475 based aluminum alloy containing zirconium instead of chromium. The mark S means a conventional 7475 aluminum alloy. The both alloys were cast into slabs as shown in **Table 2** by a standard semi-continuous direct chill technique. The slabs were homogenized at 470℃ for 10 h followed by pre-heating at 350℃ for 10 h before forging at 350℃ . In the forging stage, a sample was compressed from 100 mm high to 30 mm high. The forged samples were machined with dimensions of 30 mm high, 200 mm wide and 100 mm long. These blocks were rolled at 350℃ with re-heating at 350℃ for 1800 s after every two passes up to 4 mm thick followed by every pass up to 1 mm thick. 27 rolling passes (one pass reduction; 2 mm per pass up to 10 mm thick, 1 mm per pass up to 9 mm thick and 0.5 mm per pass up to 1 mm thick) were carried out in total and the sheets were finally prepared with dimensions of 1 mm thick and 200 mm wide.

The surface temperatures of the rolls were controlled at approximately 100 ℃ by cylindrical heaters. The roll was 160 mm in diameter and rotated 120 revolutions a minute. Commercial machine oil was used in the warm rolling process.

Regarding the alloy S, other sample sheets were also produced by conventional process in order to compare mechanical properties of the warm rolled sheets. Hot rolled plates of the alloy S were produced by conventional conditions. The plates were heated as an intermediate annealing at 480℃ for 2 h followed by furnace cooling, then rolled to 1 mm thick at an ambient temperature.

Solution heat treatment was carried out at 480℃ for 300 s followed by quenching into water immediately (T4 condition). After the quenching, artificial aging was carried out at 120℃ for 24 h (T6 condition).

Microstructure was observed using an optical microscope and a transmission electron microscope (TEM). Misorientation angles between grains were measured using electron backscattered diffraction (EBSD) equipment with a scanning electron microscope (SEM). X-ray diffraction method was used to describe incomplete pole figures, and orientation distribution functions (ODFs) were calculated from three incomplete pole figures of {111}, {110} and {100} by the harmonic method[5]. The ODFs were displayed using Bunge's system[5]. The mechanical properties of the samples in T6 condition were investigated. Tensile test specimens were got from the orientations of 0°, 45° and 90° to the rolling direction. The specimens for limiting draw ratio (LDR) measurement were annealed at 360 ℃ for 2 h followed by furnace cooling[6] (O temper) to ensure deep drawing property. LDR measurement was carried out with a punch of 33 mm in diameter under hold-down force of 3,900 N. The test method of resistance to stress corrosion cracking (SCC) in T6 condition was based on Japanese industrial standard, JIS H8711. The specimens for this test were prepared from the orientation of 90° to the rolling direction, and were immersed in a solution containing 3.5mass% sodium chloride for 10 minutes followed by drying at 25℃ for 50 minutes with addition of stress controlled at 85% of yield strength. The above cycle was repeated until the specimens were failed. The resistance to SCC was estimated by a time to failure of the specimens. Exfoliation corrosion

Table 1 Chemical composition of specimens. (mass%)

Alloy	Si	Fe	Cu	Mn	Mg	Cr	Zn	Ti	Zr	Al
M	0.02	0.03	1.64	<0.01	2.40	<0.01	5.55	0.03	0.17	Bal.
S	0.04	0.03	1.51	<0.01	2.26	0.21	5.38	0.04	<0.01	Bal.

Table 2 Experimental procedure on warm rolling.

Stage	Condition
Casting	Semicontinuous direct chill techniques into slab 100 mm×175 mm×175 mm
Homogenization	470℃-10 h
Pre-heating	350℃-10 h
Forging	350℃, 100 mm→30 mm
Machining	30 mm×200 mm×100 mm
Warm rolling	350℃, 27 passes
Annealing	350℃-30 min
Solution heat treatment	480℃-5 min W.Q.
Artificial aging	120℃-24 h

susceptibility was examined with specimens in T6 condition by immersion for 9 h in a solution containing 4M sodium chloride, 0.5M potassium nitrate, and 0.1M nitric acid at 25 ℃. The susceptibility to exfoliation was determined by visual examination according to the standard photographs in ASTM G34. Specimens of fatigue test were got from parallel to the rolling direction and machined with dimensions shown in **Fig. 1**. In this work, the axial loading fatigue test was conducted at a room temperature with the stress ratio of 0.1 and the cyclic of 30 Hz.

3. Results

3.1 Microstructure in T4 condition

Fig. 2 shows optical microstructures of warm rolled sheets after solution heat treatment. The structure of alloy M shows finer grains than that of alloy S. In alloy M, fine precipitates were confirmed in TEM observation These precipitates are identified as Al_3Zr of $L1_2$ structure tending to be coherent with the matrix **(Fig. 3a)**. This is a reason to inhibit formation of large grains. In alloy S, larger precipitates are confirmed as $Al_{18}Cr_2Mg_3$ phase **(Fig. 3b)**. These precipitates tend to be incoherent with the matrix, and they have less effect of inhibiting recrystallization.

Fig. 4 shows the estimation of microstructure formation in alloy M and S. In alloy M, many fine binary compounds inhibit formation of large grains because of coherent with matrix. On the other hand, in alloy S, large precipitates that are incoherent with matrix permit grain growth. Due to this effect, alloy M shows fine grains after solution heat treatment.

In the following sections, properties of the warm rolled sheets of alloy M are compared with that of the cold rolled sheets of alloy S.

Fig. 5 shows microstructures on both the warm

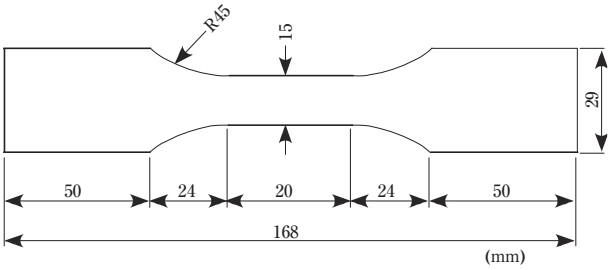

Fig. 1 Shape and dimensions of fatigue specimen.

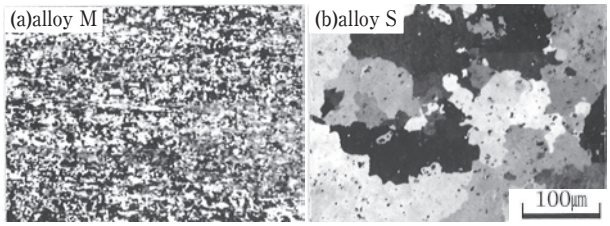

Fig. 2 Optical microstructure after solution heat treatment.

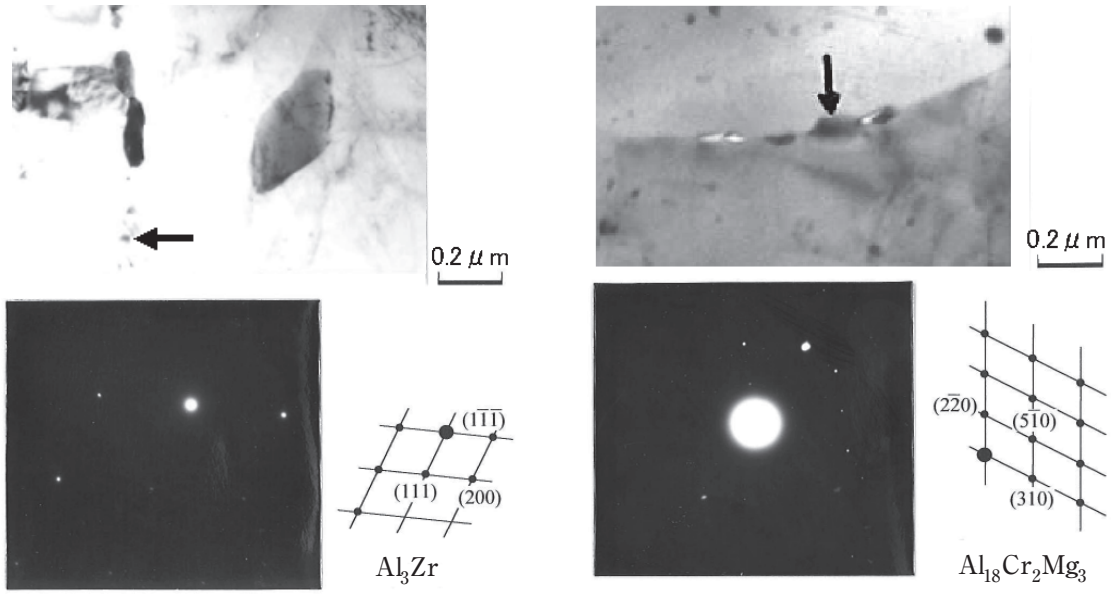

Fig. 3 TEM image and SAD pattern of alloy M and S after forging.

rolled (alloy M) and cold rolled sheets (alloy S) in T4 condition. In optical micrographs, it is found the cold rolled sheet (CR) consists of equiaxed grains about 20 μm in diameter, whereas the warm rolled sheet (WR) maintains fibrous structure as mentioned above. In TEM, it is revealed the warm rolled sheet consists of fine grains whose average diameter is approximately 3 μm. As mentioned above, fine particles are judged as Al_3Zr in alloy M (warm rolled sheet) and $Al_{18}Cr_2Mg_3$ in alloy S (cold rolled sheet).

3.2 Distribution of misorientation angle in T4 condition

Fig. 6 shows misorientation angle histograms taken from SEM-EBSD measurements. The measured area in this work was 100 × 200 μm. The warm rolled sheets have a high proportion of low angle boundary less than 15°, whereas the cold rolled sheet has a high proportion of high angle boundary. According to this measurement, it is clear the warm rolled sheet consists of subgrain structure.

3.3 Tensile properties and LDR measurements

Table 3 summarizes tensile test results in T6 condition. The tensile strength of the warm rolled sheet is about 10% higher in orientations of 0° and 90° to rolling direction than that of the cold rolled sheet, and the tensile strength in 45° direction is almost same level in the both sheets. The warm rolled sheet has an anisotropy on ductility, whereas the cold rolled sheet tends to be isotropic on it as well as tensile and yield strengths.

Fig. 7 shows the plastic strain ratio of width to thickness (Lankford value: r-value) measured at 10% elongation.

It is remarkable point that the warm rolled sheet has a quite high value over 3.5 in the orientation of 45° to the rolling direction. The warm rolled sheet also shows anisotropy on r-value. The average r-value of the warm rolled sheet is 2.2, meanwhile that of the cold rolled sheet is 0.6. The results of LDR measurements are shown in **Table 4**. The warm

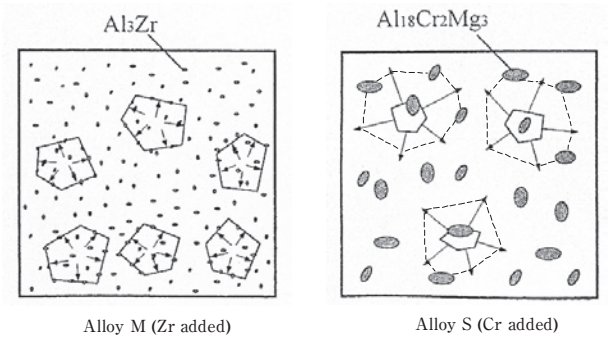

Fig. 4 Schematics of the models for the inhibiting effects of chromium and zirconium on recrystallization.

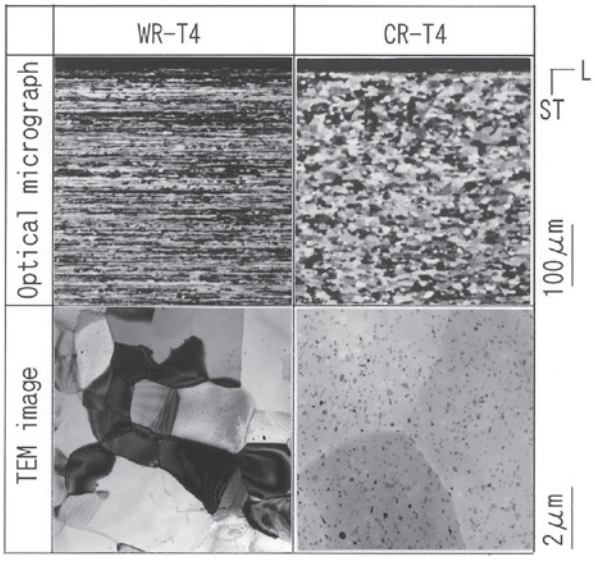

Fig. 5 Optical and TEM micrographs in T4 condition. WR : warm rolled sheet (Alloy M), CR : cold rolled sheet (Alloy S).

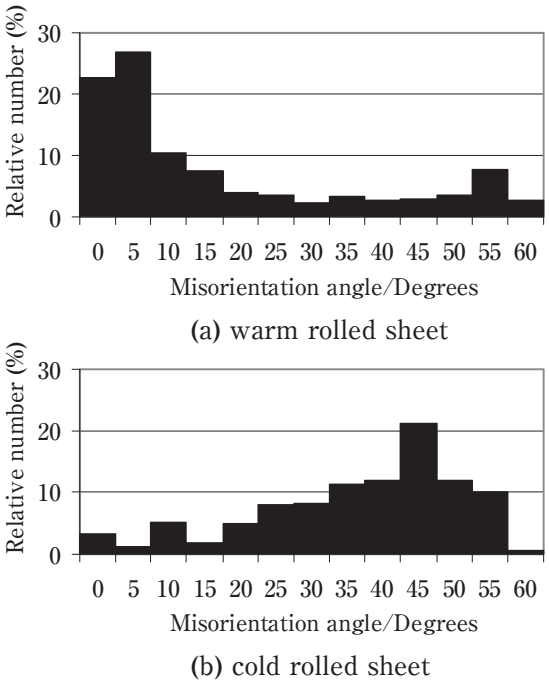

Fig. 6 Misorientation angle histograms of (a) warm rolled sheet and (b) cold rolled sheet in T4 condition.

rolled sheet tends to have a higher value than the cold rolled sheet, and it is found that the LDR values have correlation with the average r-values shown in Fig. 7.

3.4 Corrosion resistance

Fig. 8 shows the life of SCC in T6 condition. The warm rolled sheets have better resistance to SCC than the cold rolled sheets. **Fig. 9** shows the appearances and photomicrographs of the L-ST section after the immersion test. The both sheets have the same classification and are estimated of EA.

3.5 Fatigue strength

Fig. 10 gives S-N curves of the samples in T6 condition. The fatigue strength of the warm rolled sheets is about 10% higher than that of the cold rolled sheets. It is well known that fatigue strength increases with increasing tensile strength[7]. Furthermore, the effect of the fibrous structure in the warm rolled sheets on the fatigue strength should be examined in future.

Table 3 Mechanical properties of warm rolled sheet and cold rolled sheet in T6 condition.

Condition	Angle to RD	Tensile strength (MPa)	Yield strength (MPa)	Elongation (%)
Alloy M WR-T6	0°	592	496	13
	45°	522	461	19
	90°	601	455	13
Alloy S CR-T6	0°	522	461	16
	45°	521	457	17
	90°	526	468	16

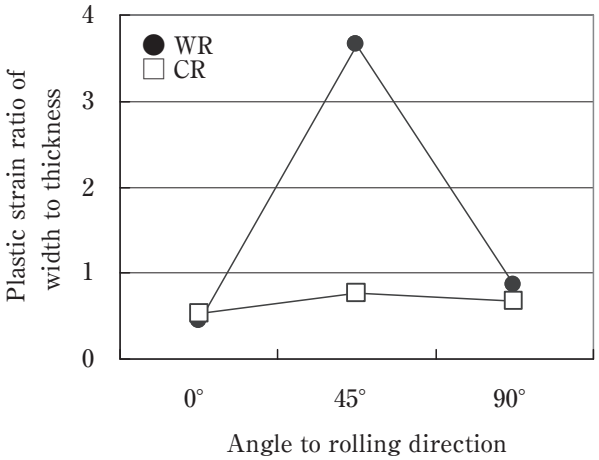

Fig. 7 Plastic strain ratio of width to thickness in T6 condition. WR : warm rolled sheet, CR : cold rolled sheet, r : average r-value.

Table 4 Limiting drawing ratio of warm rolled sheet (WR) and cold rolled sheet (CR) in O-temper.

Sample	WR	CR
LDR	2.06	2.00

4. Discussions

One of remarkable properties on the warm rolled sheets is high r-value shown in Fig. 7. According to the previous work[8] based on Taylor theory[9], it was predicted that the r-value of 45° orientation would be

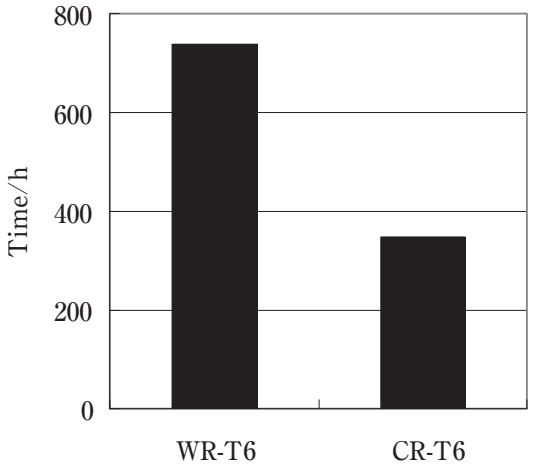

Fig. 8 Life of SCC in T6 condition. WR : warm rolled sheet, CR : cold rolled sheet.

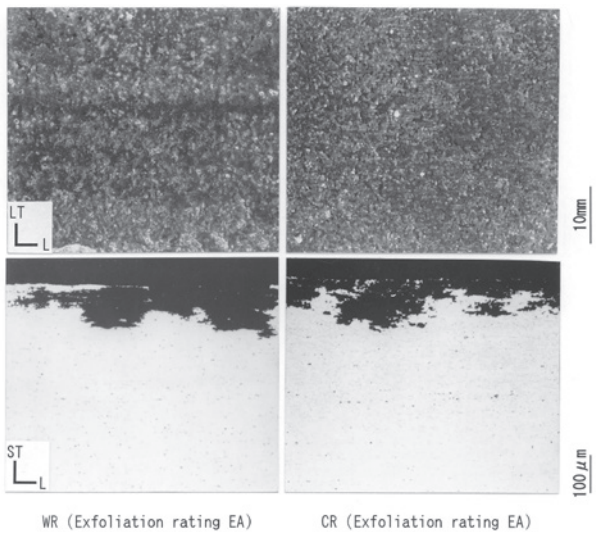

Fig. 9 Appearance and photomicrographs showing cross sections of warm rolled sheet (WR) and cold rolled sheet (CR) exposed to the test solution for 9 h.

increased by a {011}<211> Brass component. **Fig. 11** shows the ODFs at the surface layer and center layer of the samples used in this work. The {011}<211> Brass component is formed strongly through the thickness of the warm rolled sheet. Another orientation near a {123}<634> S component was perceived but its orientation density was lower than the Brass component. It is well known that β-fiber orientations involve Brass, S and C components. However, a {112}<111> C component was not perceived through the thickness of the warm rolled sheet. According to the above texture analysis, the high r-value of the orientation of 45° in the warm rolled sheet will be derived from the high orientation density of the Brass component. The present results

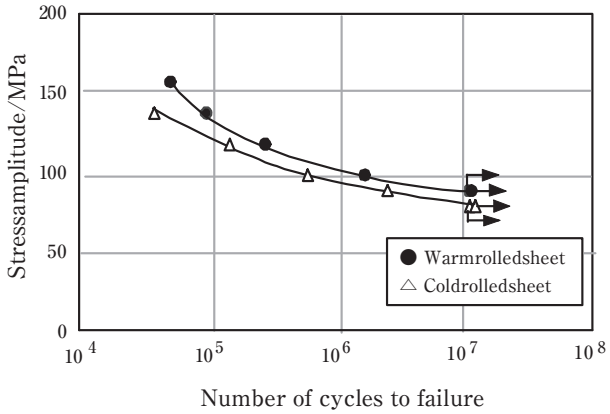

Fig. 10 Stress-number of cycle curves for the specimens in T6 condition.

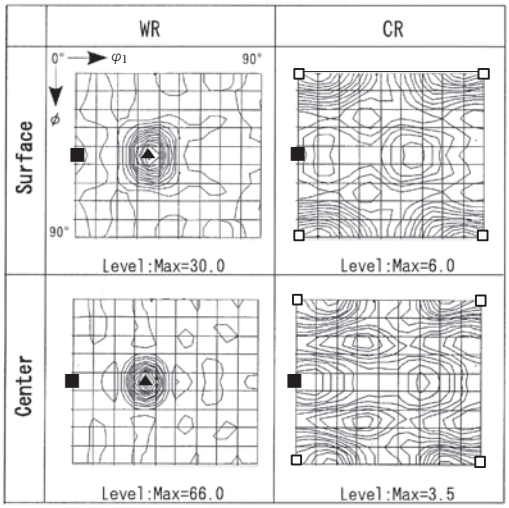

▲:Brass{011}<211> ■:Goss{011}<100> □:cube{001}<100>

Fig. 11 ODFs of warm rolled sheet (WR) and cold rolled sheet (CR) in T4 condition. (φ_2=0°).

are in agreement with the previous work[8] mentioned above. Regarding to the cold rolled sheets, as shown in Fig. 11, ND- and RD- rotated cube components as well as a {011}<100> Goss component are perceived. Their orientation densities are much lower than the Brass component in the warm rolled sheets. Besides of these quite well defined recrystallization texture components, the ODFs comprise the random component. Accordingly, the very weak recrystallization textures with the random component will lead to isotropic tensile properties of the cold rolled sheets. The cold rolled sheets consisted of β-fiber components in as rolled condition, but the orientation density of the Brass component before solution heat treatment was much lower than that of the warm rolled sheets[10]. It would be thought that the strong Brass component in the warm rolled sheets is due to the formation of fine subgrain structure that is quite stable thermally.

In the present work, specimens in O-temper were used for LDR measurements. This O-temper treatment was carried out at 360℃ after the solution heat treatment at 480℃ , so that it was confirmed the textures of specimens didn't change by the O-temper treatment. Based on this confirmation, it would be found that the average r-values have correlation with the LDR values. It would be another subject that precipitation condition may affect drawing properties, but this consideration is beyond the scope of the present work.

In the previous work[11], influence of alloy elements in 7075 aluminum alloys was investigated. It was found in the work that addition of zirconium brought about reduction of SCC life in T6 condition. The reason why the warm rolled sheets containing zirconium have good resistance to SCC may be derived from its microstructure. In the previous study on 6061 aluminum alloy extrusions[12], it was suggested the formation of a precipitate free zone (PFZ) is restrained at a low angle boundary, which leads to high resistance to intergranular corrosion. **Fig. 12** shows TEM images of the samples in T6 condition and Kikuchi patterns derived from two grains facing each other across a grain boundary. From Kikuchi pattern analysis, it was confirmed that a low angle boundary is observed in the warm rolled

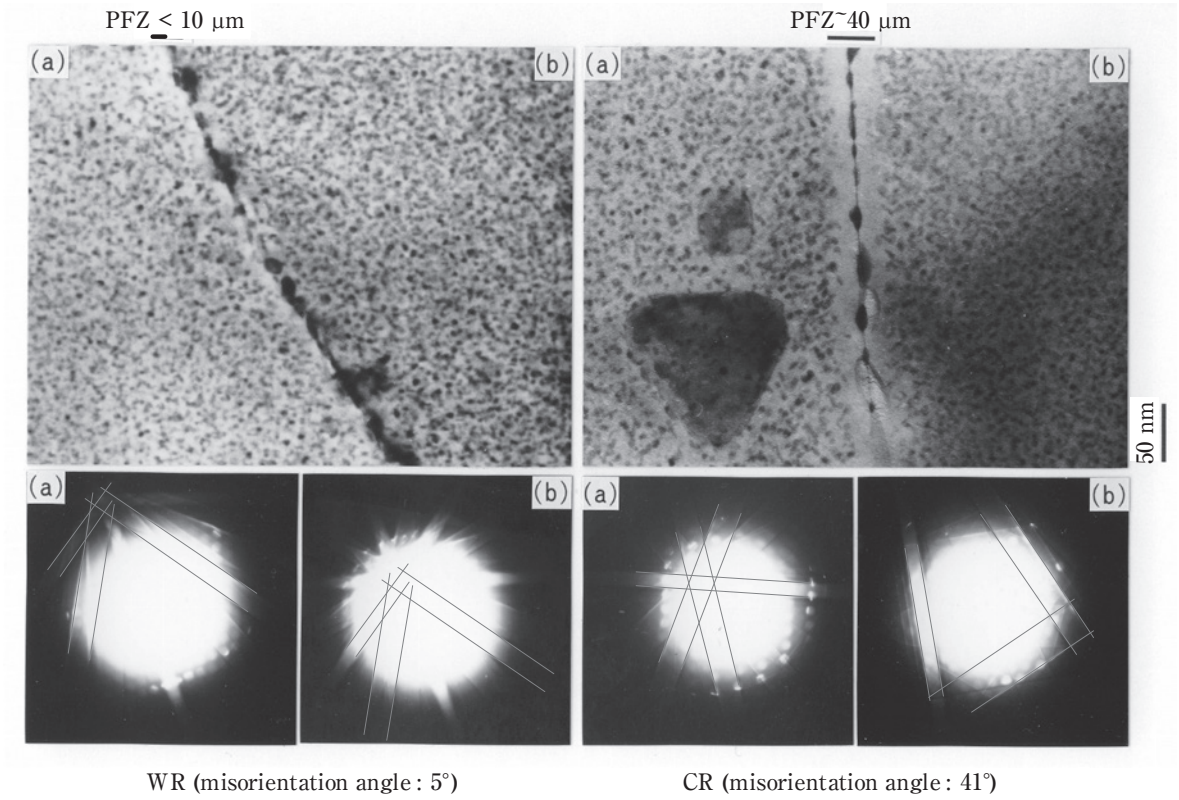

Fig. 12 TEM images and Kikuchi pattern analysis by TSL TOCA system in T6 temper.

sheet and a high angle boundary is observed in the cold rolled sheet. It is clearly found that a PFZ is restrained at the low angle boundary, whereas a PFZ is formed distinctly at the high angle boundary. Other grain boundary areas of the both sheets showed the same characteristic on the PFZ formation. In the case of narrow PFZ formation, the difference of electrochemical property between the grain boundary area and the grain interior tends to reduce, which would prevent a partial anodic reaction and lead to the improvement of resistance to SCC[13), 14)].

5. Conclusions

The mechanical properties on the warm rolled sheets of 7475 based aluminum alloy containing zirconium with fine subgrain structure were investigated comparing with conventional 7475 aluminum alloy sheets produced by cold rolling. The following points can be made:

(1) The warm rolled sheets of 7475 based aluminum alloy containing zirconium instead of chromium show fine subgrain structures after solution heat treatment. The warm rolled sheets also show the high r-value of 3.5 in the orientation of 45° to rolling direction due to well developed β-fiber components, especially with the strong {011}<211> Brass component after solution heat treatment.

(2) The average r-value of the warm rolled sheets is higher than that of the cold rolled sheets, so that the warm rolled sheets have better deep drawing properties in O-temper.

(3) PFZ is hardly formed along the low angle boundaries of the warm rolled sheets in T6 condition, which would lead to the improvement of resistance to SCC because of the uniformity of electrochemical property between the grain boundary area and the grain interior.

(4) The fatigue strength of the warm rolled sheets in the orientation of 0° to rolling direction is about 10% higher than that of the cold rolled sheets.

Acknowledgements

This work was supported in part by a research fund of the Super Aluminum Project provided by the Japan Research and Development Center for Metals

(JRCM) in the New Energy and Industrial Technology Development Organization (NEDO). The authors thank JRCM and NEDO for the permission of publication of this report.

The authors also acknowledge Professor Z. Horita, Kyushu University in Japan, for the measurements of the grain boundary misorientations by Kikuchi lines of TEM images.

References

1) E. O. Hall: Proc. Phys. Soc., **64** (1951), 747.
2) N. J. Petch: Iron Steel Inst., **25** (1953), 197.
3) The Society of Japan Aerospace Companies: Investigation for the promotion of aero parts and materials industries No. **807**, (1994).
4) H. Yoshida: Journal of Japan Institute of Light Metals, **41** (1991), 331.
5) H. J. Bunge: Texture analysis in materials science, Butterworths, (1982).
6) S. Hirano and H. Yoshida: Sumitomo Light Metal Technical Reports, **38** (1997), 95.
7) K. Takeuchi: Journal of Light Metal Welding and Construction, **4** (1966), 184.
8) H. Inoue and N. Inakazu: Journal of Japan Institute of Light Metals, **44** (1994), 97.
9) G. I. Taylor: J. Inst. Metals, **62** (1938), 307.
10) H. Tanaka, T. Minoda, H. Esaki, K. Shibue and H. Yoshida: Journal of Japan Institute of Light Metals, **52** (2002), 29.
11) The Society of Japan Aerospace Companies: Investigation for the promotion of aero parts and materials industries **No. 904**, (1995).
12) T. Minoda and H. Yoshida: Metallurgical and Material Transactions A, **33A** (2002), 2891.
13) E. N. Pough and W. R. D. Jones: Metallurgia, **63** (1961), 3.
14) Y. Murakami: Journal of Japan Institute of Light Metals, **31** (1981), 74

Hiroki Tanaka
No.3 Department, Nagoya Center, Research & Development Division, UACJ Corporation

Tadashi Minoda
Extrusion & Drawing Technology Section, UACJ Extrusion Nagoya Corporation